GLOBAL BIOCHEMICAL CYCLES, VOL. 16, NO. 1, 1009, 10.1029/2000GB001357, 2002

Study of the 1997 Borneo fires: Quantitative analysis using global area coverage (GAC) satellite data

M. J. Wooster and N. Strub
Department of Geography, King's College London, London, UK

Received 24 August 2001; revised 4 October 2001; accepted 5 November 2001; published 15 February 2002

[1] In 1997 a drought commenced in Southeast Asia, this being directly related to the then ongoing El Niño-Southern Oscillation (ENSO) event. Interaction between land clearance activities and this drought led to massive, uncontrolled vegetation fires that burned large areas of forest and agricultural land, most severely on the Indonesian island of Borneo. A similar situation in 1982–1983 led to the largest uncontrolled forest fire ever documented, damaging around 50,000 km^2 of Borneo's forest. This paper investigates the extent to which nighttime advanced very high resolution radiometer (AVHRR) global area coverage (GAC) data can be used to detail the spatial and temporal evolution of these large-scale Indonesian fire events, and particularly the 1997 activity. GAC data are a spatial subsample of the full resolution local area coverage (LAC) AVHRR data, but unlike LAC, they have been archived globally on a daily basis for almost 20 years. Despite the extreme subsampling involved in GAC data production, simulation modeling and analysis of real data indicates that surprisingly reliable fire statistics can be obtained for the 1997 Borneo fire event from GAC imagery. For three dates in October 1997 where coincident LAC and GAC data are available, once numerical adjustment for the GAC subsampling procedure is included, fire counts extracted from LAC and GAC data consistently agree to within 0.15–13%. Time series analysis of the 1997 GAC data indicates that fires began in July in south Kalimantan, principally at the interface between cleared, cultivated land and lowland rain forest. Fire activity moved generally southward and peaked in September 1997. GAC data show the equivalent of 9733 LAC pixels as containing one or more active fires on 2 September. Fire activity declined significantly in November owing to the onset of the monsoon rains, with all fires ceasing by December 1997. Analysis of the cumulative fire map distinguishes peat swamp forest as the most severely affected ecosystem on Borneo, with >20% of this land cover category being identified as directly impacted by active fires. If the performance of GAC data can be shown to extend to other El Niño years and also to less intense periods of burning, then the GAC archive offers a tool for analyzing long-term changes in the spatiotemporal pattern of fire activity in the region. Any trend can then be investigated for its relation to variations in agriculture, El Niño-related climate, and other phenomena relevant to regional change in Southeast Asia. *INDEX TERMS:* 0315 Atmospheric Composition and Structure: Biosphere/atmosphere interactions; 1610 Global Change: Atmosphere (0315, 0325); 1640 Global Change: Remote sensing; 1615 Global Change: Biogeochemical processes (4805); *KEYWORDS:* AVHRR, fires, Indonesia, Borneo, El Niño, infrared

1. Introduction

1.1. Biomass Burning in Southeast Asia (1997–1998)

[2] Biomass burning is one of the primary agents of environmental transformation in Southeast Asia. In 1997 and 1998, parts of the region were affected by very large scale vegetation fires that occurred due to interactions between land clearance activities and the anomalously dry weather conditions associated with the then ongoing El Niño-Southern Oscillation (ENSO) event. Fires particularly affected the islands of Sumatra and Borneo, where conditions were similar to those occurring during the intense 1982–1983 El Niño [*Toma et al.*, 2000]. During this earlier period the largest uncontrolled forest fire currently documented reportedly damaged around 50,000 km^2 of primary and secondary rain forest on Borneo [*Malingreau et al.*, 1985]. The 1997–1998 fires were apparently of a similar magnitude, and this degree of devastation gives significant potential for longer-term environmental degradation [*Liew et al.*, 1998]. In particular, major increases in soil erosion may result which could have a strongly negative impact on surrounding coral reefs. Furthermore, the 1997–1998 fires generated an unprecedented off-site effect in terms of the thick smog that blanketed Sumatra and Borneo and neighboring regions of Malaysia and Singapore for many months. The extensive nature of this smog and its likely effects on the environmental and human health of the region were widely reported in the media and have subsequently been examined in the scientific literature [e.g., *Legg and Laumonier*, 1999; *Levine*, 1999; *Kita et al.*, 2000]. Economic losses due to the 1997 smog alone have been estimated at >1.4 billion U.S. dollars, and >20 million people are believed to have been exposed to potentially dangerous levels of air pollution [*Brown*, 1998; *Schweithelm*, 1998]. Recently, postfire satellite-based surveys have confirmed Borneo as the Indonesian island most severely affected by the 1997–1998 fires, with fire activity being split into two intense periods of burning, separated by the 1997–1998 monsoon rains that commenced in November 1997

0886-6236/02/2000GB001357$12.00

[*Mori*, 2000]. Using quicklook imagery from the SPOT satellite, the total area of forest cleared or damaged directly by fires on Borneo has been estimated at 30,600 km^2 [*Liew et al.*, 1998].

1.2. Monitoring Active Fires With the Advanced Very High Resolution Radiometer (AVHRR)

[3] In addition to their potential for postfire damage assessment on Borneo, appropriate analysis of satellite data can also provide information on the spatial and temporal patterns of the causal fires themselves [e.g., *Wooster et al.*, 1998a; *Legg and Laumonier*, 1999; *Nakayama et al.*, 1999]. Furthermore, if appropriate data archives exist, then analysis of these fires may provide the historical perspective necessary to establish how changes in the timing, frequency, and location of burning relate to variations in ENSO-related meteorology, agricultural activity, and other relevant parameters. Only AVHRR provides data appropriate for such long-term study since it is the only suitably equipped satellite-based optical/thermal infrared imaging system to have been operating continuously for over 20 years. The AVHRR has been mounted onboard the U.S. National Oceanic and Atmospheric Administration (NOAA) TIROS-N series of Polar Orbiting Environmental Satellites (POES) since 1978. The instrument measures incoming spectral radiance in five discrete spectral channels (centered at 0.6, 0.9, 3.7, 11, and 12 μm) at a nadir spatial resolution of 1.1 km^2 and over a swath width of around 3000 km [*Kidwell*, 1995]. It has long been realized that these multispectral radiance measurements hold great value for mapping large areas of burnt vegetation and for identifying the active fires themselves. Most AVHRR-based fire detection techniques are based on the fact that subpixel hot spots greatly increase the AVHRR 3.7 μm channel brightness temperature measurement over that of the corresponding 11 μm value [*Matson and Dozier*, 1981; *Robinson*, 1991]. Simple thresholding of the 3.7–11 μm brightness temperature difference, or some adaptation of this technique, can thus identify AVHRR pixels containing active fires [e.g., *Matson and Dozier*, 1981; *Flasse and Ceccato*, 1996; *Giglio et al.*, 1999]. Combined with the large swath width of the AVHRR sensor, this approach allows regional scale fire analysis that would be impossible using nonremote sensing methods [*Matson and Holben*, 1987; *Robinson*, 1991]. Unfortunately, however, the POES data holding capacity limits storage of the full spatial resolution AVHRR local area coverage (LAC) data to only 10% of each Earth orbit, making AVHRR LAC observations of any particular Earth location generally patchy in both space and time. Since all LAC data are transmitted from the POES satellite as a real-time direct broadcast, one solution to this problem is to rely on a locally installed AVHRR receiving station to obtain data from each relevant satellite overpass [*Flasse et al.*, 1997; *Legg and Laumonier*, 1999]. Such stations have been shown to be very effective, but they do not provide data prior to the receiving station installation date and so cannot assist in providing long-term historical data coverage.

[4] Fortunately, to ensure complete AVHRR Earth coverage, a spatial subsampling procedure is applied on board the POES satellite so that each entire orbit of data is retained in a spatially degraded form known as AVHRR global area coverage (GAC). The full GAC data take is downloaded from each POES orbit and appropriately archived by NOAA, thus providing historical, repetitive whole-Earth coverage with a daily repeat cycle [*Cracknell*, 1997]. The spatial coverage of a single AVHRR LAC or GAC scene is illustrated in Figure 1, though because of the satellite data storage limitations, only the GAC scene maybe present in the data archive. The LAC-to-GAC subsampling process involves pixel averaging and pixel skipping and produces a product greatly reduced in data volume, with GAC pixels having a 4 × 1.1 km spatial resolution and a 3 km gap between each scan line (Figure 2). The clear disadvantage is that this subsampling lessens the AVHRR data content and quality, but it means that the full GAC data set is archived and is becoming freely available through the NOAA Satellite Active Archive facility (http://www.saa.noaa.gov). There is thus the potential for investigating longer-term variability in large-scale biomass burning patterns with these data [*Barbosa et al.*, 1999a, 1999b].

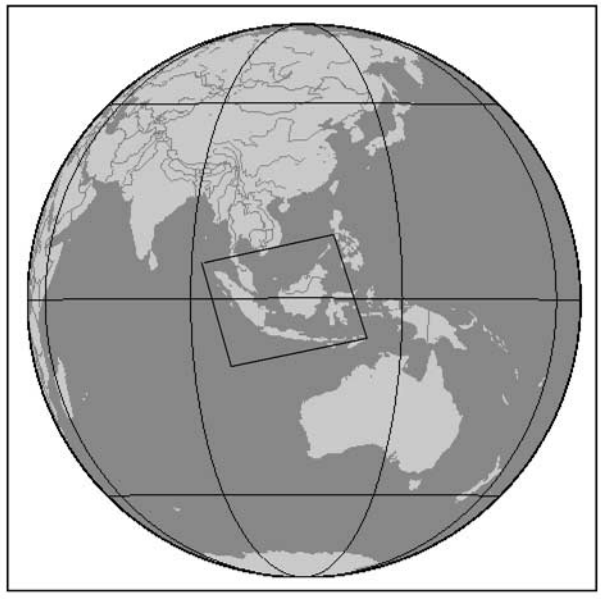

Figure 1. Spatial coverage of an AVHRR scene in relation to Southeast Asia. Coverage shown is that which is most effective for Indonesia. A LAC scene covers this area with 2048 × 2048 pixels, with the corresponding spatially subsampled GAC scene being 410 × 682 pixels.

[5] In certain forested regions where burnt areas maybe spatially patchy the detail revealed by GAC data may be insufficient for accurately and effectively mapping fire-affected area. However, the very high sensitivity of the AVHRR 3.7 μm channel measurement to the presence of even quite small hot spots means that pixels incorporating active fires are still quite apparent in GAC data, despite the severe subsampling involved (Figure 2). GAC data have already been used to investigate the seasonality and long-term burning patterns of active fires on the African continent [*Cooke et al.*, 1996]. As highlighted by *Robinson* [1991], however, further region-specific investigations must take place to determine the exact effect of the GAC subsampling procedure on the data's ability to discriminate these phenomena in different environments. Certain of the African studies have suggested that the quantitative information provided by GAC is actually of rather poor quality, distinguishing perhaps only a few percent of the fires identifiable in full-resolution LAC imagery [*Belward et al.*, 1994]. However, under the environmental conditions pertaining to Southeast Asia, GAC data may perform somewhat differently. Prior to any analysis of the historical GAC archive of the region, the quality of the fire-related information derived from the GAC imagery must therefore be investigated. This paper describes results of this analysis for the severe El Niño-related fire event of 1997, concentrating on the island of Borneo, where the majority of the forest damage took place.

2. The 1997 Borneo Fires

[6] Borneo is the third largest island in the world and covers an area of 755,000 km^2, being situated southeast of the Malay

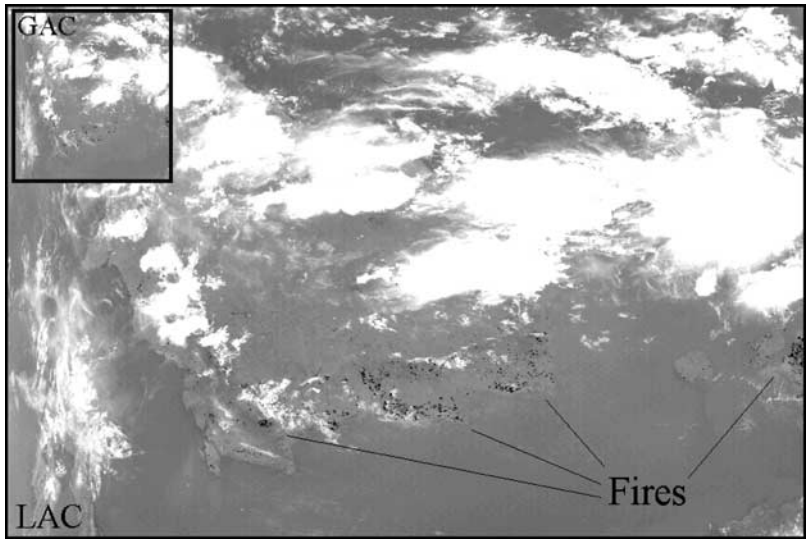

Figure 2. Nighttime LAC and GAC data for the area depicted in Figure 1. Data are from the AVHRR 3.7 μm channel, and the scene data are 12 October 1997. Data are presented in proportion to their actual digital data volumes, giving a LAC:GAC ratio of 15:1. The GAC sampling process consists of averaging four out of five LAC pixel measurements along the scan line (i.e., skipping one along-scan pixel in every five) and selecting data from every third scan only. Thus only 27% of the LAC pixels actually contribute to the GAC pixel data and each GAC pixel is an average of four LAC measurements. A gray scale palette has been applied to display clouds (low temperature) as white and fire-affected pixels (high temperature) as black. Fires are evident in the south of Borneo and Sumatra in both data sets.

Peninsula (Figure 3). Politically, the island is divided between Indonesia (Kalimantan, population 9 million), the Malaysian Federation (Sarawak and Sabah, population 3 million) and the Islamic Sultanate of Brunei (population 260,000). Large areas of Borneo are covered by dense rain forest vegetation, particularly lowland *Dipterocarp* forest, though much has been degraded by commercial logging operations. Significant areas of industrialized agriculture have been established in recent decades, and "slash and burn" is being used annually to extend the area available for new agriculture. Burning is also used to prepare existing agricultural land for new planting before the rains. Mean annual rainfall for the island is 3800 mm, and rainfall is distributed over two distinct seasons, the monsoon (normally between October and March) and a relatively drier summer period for the rest of the year. In 1997, however, the summer was significantly drier than normal, with rain being totally absent at some locations for many weeks. These conditions were similar to those experienced during the 1982–1983 drought and are in stark contrast to the normal summer rainfall pattern, where rainless periods longer than a few days are relatively rare [*Toma et al.*, 2000]. Figure 4 shows sample rainfall station data for 1997–1998, and *Toma et al.* [2000] provide further information on the longevity and intensity of the 1997 drought. As in 1982–1983, the anomalous 1997 meteorological conditions were directly related to the ongoing ENSO event, which was reportedly the most intense this century [*Gutman et al.*, 2000]. The ENSO-related drought allowed burning on Borneo to become much more widespread in 1997 and 1998 than in nondrought years. The result was the massive forest damage reported by *Liew et al.* [1998] and *Mori* [2000]. Certain of the 1997–1998 forest fires have been analyzed using AVHRR LAC imagery and similar data from the ERS Along Track Scanning Radiometer [e.g., *Buongiorno et al.*, 1997; *Nakayama et al.*, 1999; *Legg and Laumonier*, 1999; *Siegert and Rücker*, 2000; *Siegert and Hoffmann*, 2000; *Fuller and Fulk*, 2000]. *Wooster et al.* [1998a] have shown how AVHRR GAC data can effectively illustrate the broad spatial distribution of the Borneo fires, but the current study is the first detailed investigation of the GAC data content and their quantitative ability to discriminate active fires in this region.

3. Capability of GAC Data to Identify Active Fires

3.1. Theoretical Modeling

[7] GAC data are constructed by taking data from every third AVHRR scan, averaging the data from every four along-scan LAC pixels, and skipping the fifth [*Kidwell*, 1995; *Belward et al.*, 1994]. Clearly, the along-track, scan line skipping procedure means that any fire signals present in the discarded scan lines will be totally absent from the resultant GAC data set. However, since the spatial distribution of fires should not be confined to a regular pattern of AVHRR scan lines, the GAC data can be treated as a simple one-third sample in this regard, and the equivalent LAC along-track statistical distribution of fire pixels can easily be reconstructed [*Belward et al.*, 1994]. What is more critical is how the along-scan averaging procedure affects the ability of GAC data to discriminate fire-affected pixels. To investigate this, a simple model of the AVHRR measurement process was used to study the effect of the GAC along-scan spatial subsampling. The model simulated AVHRR LAC spectral radiances ($L_{3.7}$ and L_{11}) given an observed surface with a particular temperature and the presence or absence of a subpixel fire hot spot, again with particular size and temperature characteristics. For simplicity, no atmospheric or emissivity effects were included in the simulation. Numerical equations used were based on the two-component, area-weighted Planck functions originally described by *Matson and Dozier* [1981] ((1) and (2)). As outlined by *Robinson* [1991], these equations have previously been

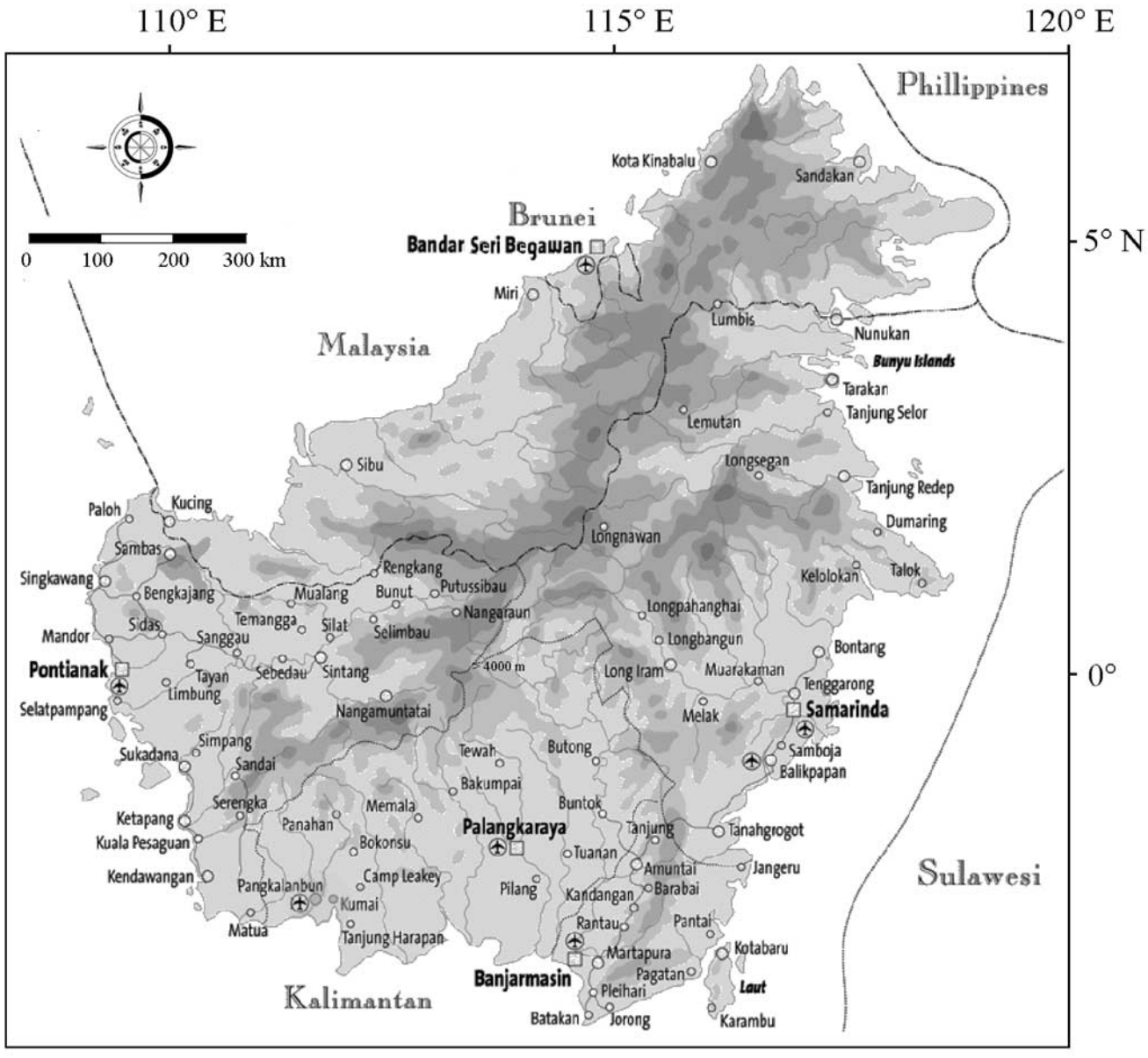

Figure 3. Map of Borneo which contains territory of Malaysia (Sarawak and Sabah), Indonesia (Kalimantan), and Brunei. Kalimantan is further subdivided into western, eastern, and southern regions. Borneo is a mountainous island, with a dorsal range rising to a maximum elevation of 4101 m at Mount Kinabalu in the far northwest. Topography is depicted here in five gray scales, each equivalent to 1000 m height increments.

inverted with real AVHRR data and used to estimate the size and temperature of subpixel fires.

$$R_{3.7} = \frac{S_h}{A} L_{3.7}(T_h) + \frac{(A - S_h)}{A} L_{3.7}(T_c) \quad (1)$$

$$R_{11} = \frac{S_h}{A} L_{11}(T_h) + \frac{(A - S_h)}{A} L_{11}(T_c), \quad (2)$$

where $R_{3.7}$ is the modeled spectral radiance in the AVHRR 3.7 μm channel (W m^{-2} $sr^{-1}$$\mu m^{-1}$), R_{11} is the modeled spectral radiance in the AVHRR 11 μm channel (W m^{-2} sr^{-1} μm^{-1}), S_h is the planimetric area of the fire (m^2), A is the AVHRR pixel area (m^2), $L_{3.7}(T)$ is the spectral radiance emitted in the AVHRR 3.7 μm channel by a body at T Kelvin (W m^{-2} $sr^{-1}$$\mu m^{-1}$), $L_{11}(T)$ is the spectral radiance emitted in the AVHRR 11 μm channel by a body at T Kelvin (W m^{-2} sr^{-1} μm^{-1}), T_h is the fire temperature (K), and T_c is the ambient background surface temperature (K).

[8] Spectral radiances from four simulated "neighboring" LAC pixels were averaged to obtain a single GAC pixel measurement. The simulation was carried out repeatedly, with the number of LAC pixels containing active fires varied between one and four to determine the effect on the resultant GAC pixel measurement. The LAC and GAC data sets were then converted from spectral radiance into brightness temperature units ($T_{3.7}$ and T_{11}) using the inverse Planck function procedure outlined by *Wooster et al.* [1995]. The difference between the corresponding 3.7 and 11 μm brightness temperatures ($T_{3.7\text{-}11}$) was then calculated since this is

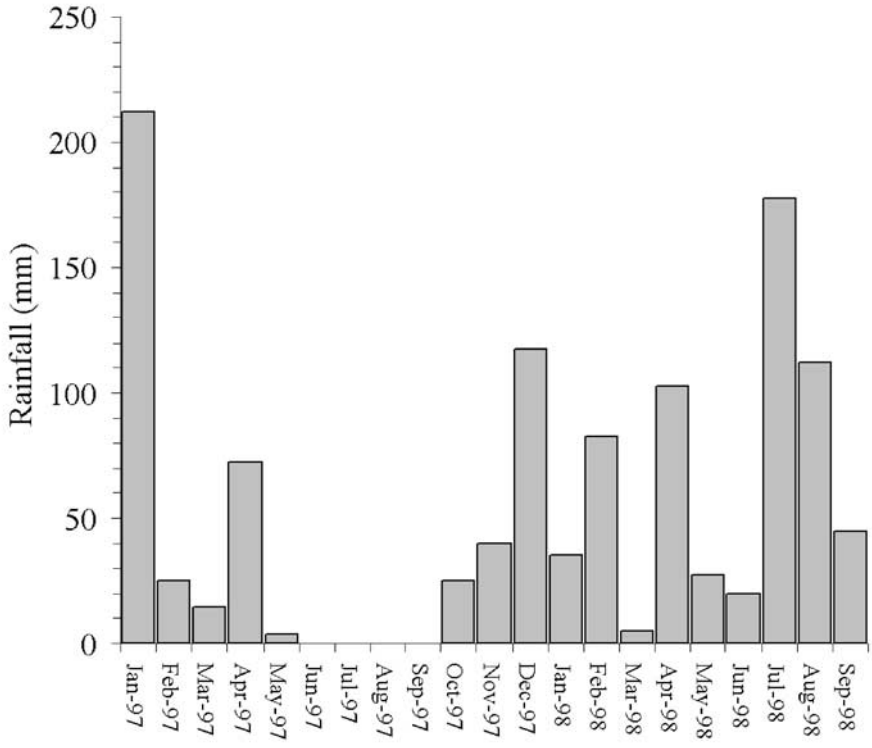

Figure 4. Rainfall data for 1997–1998 for the airport meteorological station at Banjarmasin, south Kalimantan (3°20′S, 114°35′E), whose location can be seen in Figure 3. This southern region of Borneo is one of the most severely affected by the 1997 fires. The lack of rainfall during June–September 1997 is clearly evident, contrasting sharply with the same period the following year.

the most important discriminatory parameter used in AVHRR fire detection techniques. As outlined previously, the differential response of the AVHRR 3.7 and 11 μm channels to subpixel hot spots causes the value of $T_{3.7\text{-}11}$ to rise sharply in the presence of a fire [*Matson and Dozier*, 1981; *Robinson*, 1991]. At nonfire "background" pixel locations, (1) and (2) indicate $T_{3.7\text{-}11}$ to be zero; however, in real AVHRR data the spatially and spectrally varying atmospheric transmissivity and surface emissivity typically mean background $T_{3.7\text{-}11}$ values of 0.5–5 K. Thus, for a pixel containing an active fire the value of the $T_{3.7\text{-}11}$ parameter over and above the natural background variation is directly related to the capability for discriminating that pixel as "fire affected." The larger the $T_{3.7\text{-}11}$ increase, the more unambiguous the hot spot identification.

[9] Results from the modeling are shown in Figure 5. As would be expected, when all four contributing LAC pixels include an active fire, the resultant GAC pixel signal is identical to the individual LAC pixel measures. However, while lowering the number of LAC pixels containing active fires does reduce the corresponding GAC $T_{3.7\text{-}11}$ measure, because of the nonlinear and logarithmic relationships involved in (1) and (2) the variables are not reduced in direct proportion. For example, when the LAC fire pixel $T_{3.7\text{-}11}$ measure is 40 K the equivalent GAC measure would still be 17 K even if only one fire pixel were included in the four contributing LAC pixels. Increasing the number of LAC fire pixels included in the GAC pixel measure increases the GAC $T_{3.7\text{-}11}$ measure further (Figure 5). The relationships are relatively insensitive to either the background or fire temperature, providing evidence that fire analysis based on AVHRR GAC data could be a relatively reliable tool in many circumstances. However, inspection of the model results also confirmed that because of the four-pixel averaging used to derive GAC data, for any particular fire temperature and $T_{3.7\text{-}11}$ detection threshold, the smallest detectable fire in a GAC pixel is still four times larger than the smallest detectable fire in a LAC pixel.

[10] The model indicates that AVHRR GAC data are clearly theoretically capable of identifying active fires, perhaps more so than initially might be thought given the extreme subsampling involved. However, it was noted that the simple modeling performed here did not incorporate simulation of the AVHRR point spread function or spatial autocorrelation, which are important when analyzing real data [*Breaker*, 1990; *Wooster et al.*, 1998b]. Thus, having proved that GAC data are theoretically capable of effectively detecting active fires under a number of scenarios, the capacity of the data for this purpose was further tested using a series of real data intercomparisons.

3.2. Test Using Real Data

[11] This analysis of AVHRR data concentrated on nighttime scenes only since daytime fire detection presents more complex issues due to the additional component of 3.7 μm solar radiation being reflected from clouds, water bodies, and other image features [*Robinson*, 1991]. Many previous AVHRR LAC fire studies have concentrated solely on nighttime data [e.g., *Lee and Tag*, 1990; *Langaas*, 1992, 1993; *Legg and Laumonier*, 1999], but daytime LAC detection methods are now also well established. *Justice and Dowty* [1994] and *Giglio et al.* [1999] review many of these procedures. For the current study it was felt that use of daytime data would add a further and unnecessary complication since the primary purpose was concerned with evaluating the effect of the GAC subsampling procedures on fire detection capability. Daytime GAC fire detection would be prone to increased error from the

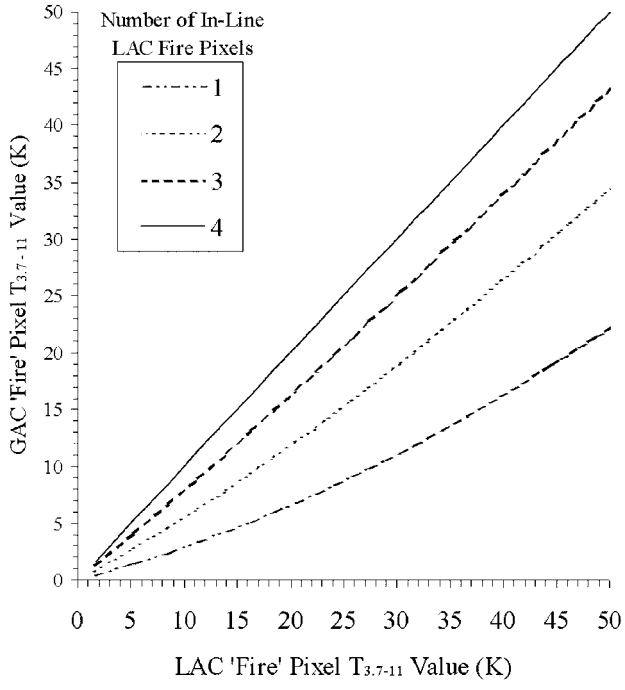

Figure 5. Comparison of the 3.7−11 μm brightness temperature difference ($T_{3.7\text{-}11}$) for simulated AVHRR LAC and GAC pixels modeled to contain active fires. For this simulation the background temperature was set to 15°C, and the fire temperature was set to 800°C. LAC pixel spectral radiances were modeled using (1) and (2), and the equivalent GAC pixel spectral radiance was constructed by averaging signals from four simulated LAC pixels, between one and four of which were modeled to contain an active fire. Radiances were converted to brightness temperatures prior to calculation of the $T_{3.7\text{-}11}$ parameter. Under the conditions modeled the AVHRR sensor would saturate when $T_{3.7\text{-}11}$ reached ~50 K.

effect of solar-reflected radiation increasing the $T_{3.7\text{-}11}$ signal at certain nonfire pixels. Thus the current study was implemented using the simplest nighttime case. Use of daytime data may, of course, be important in discriminating the shorter-lived agricultural fires that may only be active during the day and which may even dominate burning in non-El Niño years [*Eva and Lambin*, 1998]. However, the 1997 Borneo fires are reported to have been generally large, long-lived events, and following the reasoning of *Legg and Laumonier* [1999], the use of nighttime data was thus considered appropriate.

[12] Using the Satellite Active Archive, three dates in October 1997 were identified where fires existed on Borneo under relatively cloud-free conditions and where both GAC and LAC versions of the same nighttime data existed. Cloud-contaminated pixels were first screened out using a simple 11 μm temperature threshold [*Robinson*, 1991]. Following most previous AVHRR fire studies, the fire pixel detection tests were based on thresholding of the $T_{3.7\text{-}11}$ data values, and two specific methods were tested. The first approach was based on use of a single, image-wide $T_{3.7\text{-}11}$ threshold, following, for example, *Kaufman et al.* [1990], *Robinson* [1991], *Kennedy et al.* [1994], and *Buongiorno et al.* [1997]. The second "contextual" approach involved "potential" fire pixels being identified using a single, image-wide $T_{3.7\text{-}11}$ threshold, but then these pixels were confirmed or rejected as "true" fire pixels based on comparison of their actual $T_{3.7\text{-}11}$ value with those of the immediately surrounding background pixels [*Justice and Dowty*, 1994]. The specific contextual algorithm implemented was that of *Flasse and Ceccato* [1996], adapted to the particular conditions encountered on Borneo following *Nakayama et al.* [1999]. Though apparently successful when applied to the LAC data sets, the contextual method provided poor results when tested on the corresponding GAC imagery, failing to detect many fire-affected pixels that could clearly be discriminated by visual inspection. Investigation showed that this failure was due to the contextual aspect of the procedure where, as outlined by *Flasse and Ceccato* [1996], the $T_{3.7\text{-}11}$ threshold is altered as a function of the standard deviation of the $T_{3.7\text{-}11}$ background pixel values. The background pixel $T_{3.7\text{-}11}$ standard deviation is noted to be much higher for a set number of GAC pixels than for the same number of LAC pixels owing to the averaging of four LAC pixels into every GAC measurement. This makes the GAC $T_{3.7\text{-}11}$ threshold returned by the contextual filter anomalously high, and this precludes many obviously fire-affected GAC pixels being confirmed as such by the second stage of the contextual technique. Consequently, the contextual algorithm performs poorly in this case.

[13] The spatially varying thresholds of the contextual approach are more obviously required during analysis of daytime imagery, where solar heating and solar-reflected radiation typically lead to a higher spatial variability in the 3.7 μm brightness temperature background. The apparent deficiency of the contextual approach for GAC analysis and the use of solely nighttime data led our study to adopt the simple, image-wide thresholding approach for all further processing. Each LAC and GAC scene was thus subject to a fire detection test based on thresholding of the $T_{3.7\text{-}11}$ parameter. Analysis of the $T_{3.7\text{-}11}$ histograms confirmed the relative similarity of this parameter in the LAC and GAC data sets (Figure 6) and indicated that the appropriate threshold for identifying fire-affected pixels was somewhere above 5 K. Detection of hot spot (fire) pixels within each image was attempted five times, varying the $T_{3.7\text{-}11}$ threshold between 6 and 10 K in order to optimize the method. On each run, AVHRR pixels having $T_{3.7\text{-}11}$ values above the chosen threshold were classified as containing active fires (i.e., fire affected). Fire count statistics were then extracted, and following *Belward et al.* [1994], the inverse of the GAC subsampling procedure was applied to the GAC fire pixel counts so that results from contemporaneous GAC and LAC scenes could be meaningfully compared. This simply involved correcting the GAC fire counts for the 27% sampling factor used when deriving GAC data and multiplying the resultant fire counts by 4 to take into account the fact that each GAC pixel is originally derived from four LAC measurements [*Belward et al.*, 1994].

[14] Results from these procedures are shown in Figure 7 and indicate a strong correspondence between the number of fire pixels identified in the corresponding LAC and GAC imagery. The relationship is reasonably consistent over all image dates and detection thresholds tested. Analysis also confirmed that the spatial distribution of the LAC fire pixels was effectively reproduced by the GAC imagery, though obviously with a loss of spatial detail. As expected, when using the highest $T_{3.7\text{-}11}$ threshold (10 K), the number of identified fire pixels is at a minimum. At this threshold, there is also only a 3% variation in the number of LAC fire pixels detected between the individual image dates, and importantly, the difference between the number of fire pixels detected in corresponding LAC and GAC images consistently lies within a small −3 to +3% range. However, visual inspection of the imagery confirms that use of the 10 K threshold precludes detection of many fire pixels. When using a lower $T_{3.7\text{-}11}$ threshold of 6 K, similar inspection confirms a much stronger agreement between visual and automated fire pixel identification. At this threshold, fire pixel counts are at a maximum, and there is a 20% variation between counts on different image dates. Crucially, however, there is still only a relatively small difference between the fire pixel

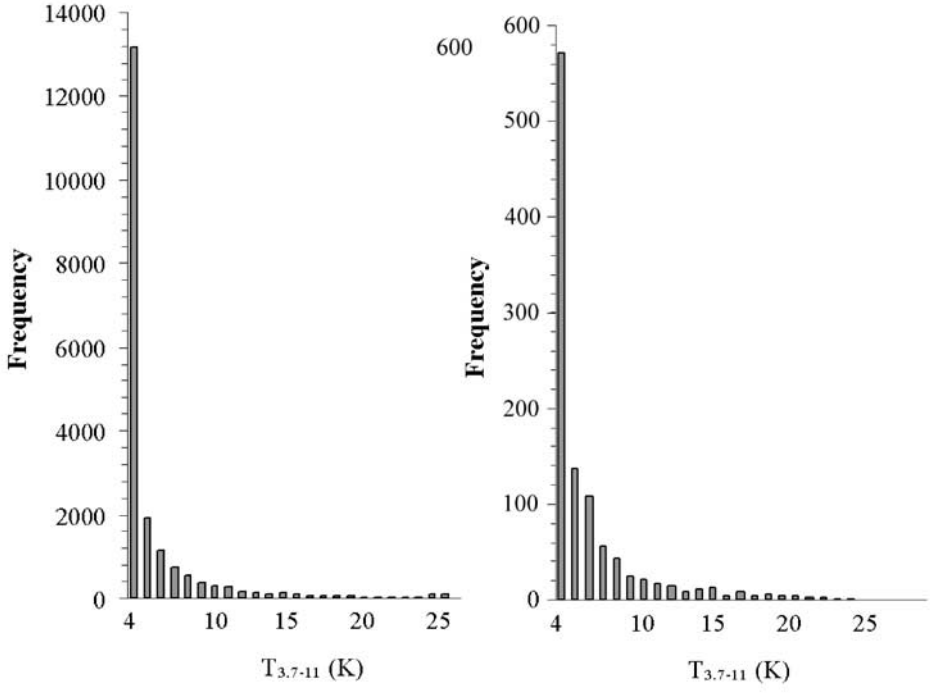

Figure 6. Comparison of the 3.7–11 μm brightness temperature difference measure ($T_{3.7\text{-}11}$) for Kalimantan, Borneo, for 12 October 1997, observed in AVHRR LAC and GAC data. Cloudy pixels were masked using a simple 11 μm channel brightness temperature threshold, and pixels having $T_{3.7\text{-}11}$ <4 K are not shown.

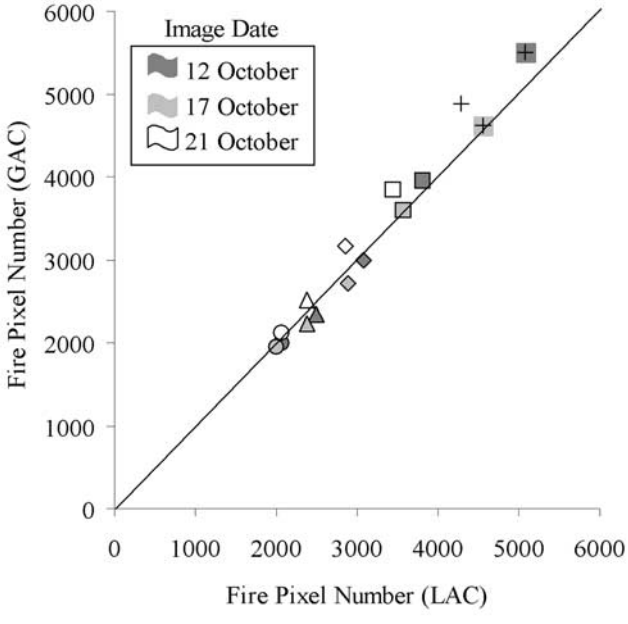

Figure 7. The number of fire pixels identified in corresponding nighttime AVHRR LAC and GAC data of Borneo for three dates in October 1997. Each scene was relatively cloud free in the fire-affected area and was analyzed using a series of temperature thresholds for the $T_{3.7\text{-}11}$ "fire pixel" detection test. Threshold values are indicated by the symbols: plus, 6 K; open square, 7 K; open diamond, 8 K; open triangle, 9 K; open circle, 10 K, while image date is indicated by shading given in the legend. The 1:1 correspondence line is shown.

counts extracted from temporally coincident LAC and GAC data, ranging from 0.15 to 13%. GAC data therefore appear to provide a reasonably reliable record of fire pixel number under these conditions. A further decrease in the $T_{3.7\text{-}11}$ threshold to 5 K results in the incorrect classification of many obviously nonfire pixels, particularly on the 21 October 1997 image. As previously stated, in the high humidity and smog-affected atmosphere of Borneo a top-of-atmosphere $T_{3.7\text{-}11}$ value of this magnitude can be generated by atmospheric effects alone. This accounts for the errors of commission when using a 5 K threshold, and a $T_{3.7\text{-}11}$ threshold of 6 K was therefore chosen for the remainder of the study.

[15] It is worth considering why the agreement between the LAC and GAC fire statistics of Borneo appear so strong. Specifically, why are the data in much better agreement than are corresponding data sets for West Africa, where *Belward et al.* [1994] found that GAC data simulated from daytime LAC scenes severely underestimated fire pixel number? To help answer this, we can consider conditions in two different ecosystems; ecosystem 1, which favors small fire sizes, and ecosystem 2, where conditions favor the generation of much larger fires (Figure 8). Ecosystem 1 might correspond broadly to the West African ecosystems analyzed by *Belward et al.* [1994] during relatively normal climatic conditions, while ecosystem 2 is likely to more closely resemble the degraded Indonesian forest under the El Niño-related drought conditions encountered during the current study. Assuming a constant fire and background temperature, application of any particular $T_{3.7\text{-}11}$ threshold to AVHRR data of either ecosystem will directly translate to the same minimum detectable fire size. As outlined in section 3.1, this minimum detectable fire size will be 4 times larger for GAC than for LAC data. For example, results from the model used in section 3.1 indicate that use of a 10 K $T_{3.7\text{-}11}$ threshold results in a minimum detectable fire size of 50 m^2 for LAC data and 200 m^2 for GAC data in either ecosystem. This assumes an 800°C fire, a 30°C background, and the absence of

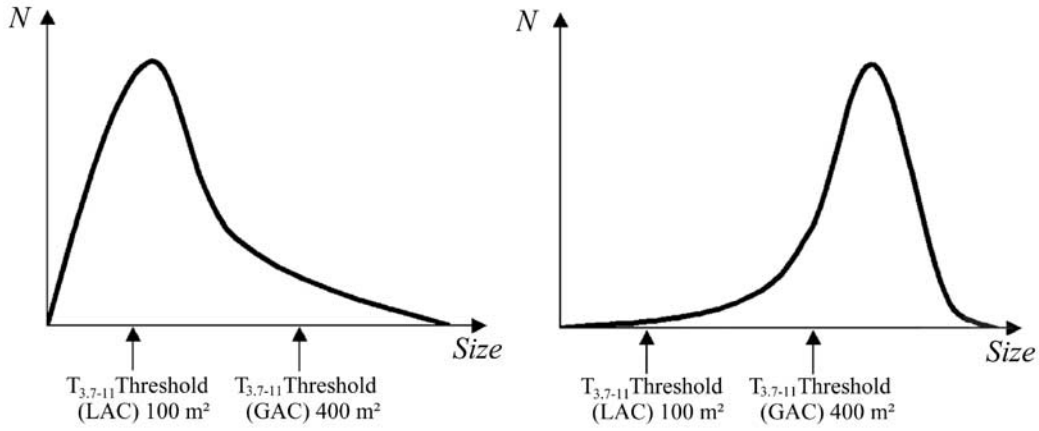

Figure 8. Theoretical fire size distributions for two different ecosystems. As illustrated here, assuming a constant fire temperature, application of any particular $T_{3.7\text{-}11}$ threshold to AVHRR data of these areas will directly translate to a minimum detectable fire size for that ecosystem, with this size being 4 times larger for GAC data than for LAC data.

atmospheric and surface emissivity effects, so these minimum detectable fire sizes would be somewhat increased in real data because of the presence of these effects. Comparing theoretical fire detection rates in ecosystem 1 and 2, Figure 8 indicates that in both ecosystems the majority of the fires are >50 m^2 and are thus detectable using AVHRR LAC data with the 10 K $T_{3.7\text{-}11}$ threshold. However, in ecosystem 1 the majority of fires are <200 m^2 and so are missed when using AVHRR GAC data with this detection threshold. This is not the case for ecosystem 2, which favors the development of fires larger than the 200 m^2 minimum detectable fire size of GAC data, and thus the GAC fire detection rates are much closer to those obtained with LAC data in this ecosystem. The fact that the drought-stricken forest of Borneo favored the development of very large fires, whereas the West African ecosystems studied by *Belward et al.* [1994] generally favored much smaller fires, is one explanation for the much stronger agreement between LAC and GAC fire counts found in the current study.

[16] A further reason for the comparatively poor fire detection performance reported by *Belward et al.* [1994] for GAC data of West Africa is the use in that study of a hot spot identification method incorporating a requirement that the 3.7 μm brightness temperature itself must exceed 320 K. This test was introduced largely so that any GAC pixels identified as fire affected would be directly comparable across the sahelian grassland, bush savanna, and Guineo-Congoilan forest zones present in that study region [*Belward et al.*, 1994, Figure 3]. However, use of a 320 K 3.7 μm threshold effectively means that all four in-line LAC pixels that go into constructing any particular GAC pixel must themselves all be fire pixels if the resulting GAC pixel is also to be classed as a fire. Any GAC pixel containing fewer than four individual LAC fire pixels will thus not be classified as a hot spot using this methodology. In West Africa the occurrence of four in-line LAC fire pixels is much more likely in the savannah environment, where fires extend over an often relatively long and linear fire front. The West African forest fires noted by *Belward et al.* [1994] tended to be characterized more by individual LAC hot spot pixels. Thus *Belward et al.* [1994] found agreement between LAC and GAC fire counts to be worst in the forested regions and best in the savanna. For Borneo, however, the climate and ecosystem type is far less varied than that of West Africa, and no 3.7 μm threshold test was required for effective hot spot detection. Detection of fire pixels was based solely on thresholding of the $T_{3.7\text{-}11}$ data, and Figure 5 indicates that with this technique many GAC pixels comprised of less than four fire affected LAC pixels will still themselves be identified as hot spots when using an appropriately low threshold. This is a further factor that explains the increased proportion GAC fire pixels correctly identified as hot spots in the current study when compared to that of *Belward et al.* [1994].

[17] The disadvantage of the approach used here is that without use of the 320 K 3.7 μm threshold test of *Belward et al.* [1994], we do not know exactly how many of the original LAC pixels comprising the resultant GAC measure actually contained a fire. By applying the inverse GAC data averaging procedure of *Belward et al.* [1994] to compare the LAC and GAC fire statistics we are inherently assuming that for every GAC hot spot pixel detected, there were, on average, four LAC hot spot pixels. Detailed analysis of an AVHRR LAC scene (12 October 1997) confirms that the majority grouping of LAC fire pixels is, in fact, an along-scan group of four, thus confirming the preponderance of larger fires under this ecoclimatic condition. However, owing to the hot spot sensitivity of the 6 K $T_{3.7\text{-}11}$ threshold many of the GAC fire pixels clearly cannot have had all four contributing LAC fire pixels as fire affected. Nevertheless, the strong agreement between the 1997 LAC and GAC fire counts (Figure 7) indicates that in these conditions the overestimate introduced by the applying the times 4 factor to the GAC fire counts is broadly balanced by the underestimate introduced by the failure to identify GAC fire pixels having a fire size smaller than the minimum detectable threshold (Figure 8). When analyzing longer multiyear time series, it would be necessary to consider whether the fire size distribution is constant or whether it changes from year to year. It seems likely that fire size distribution will be very different between El Niño and non-El Niño years, but between the various El Niño years covered by the GAC archive a more constant distribution might be expected. Multiyear LAC-to-GAC comparisons or analysis of high spatial resolution imagery would be required to confirm this situation.

[18] Finally, it should be noted that despite the early findings of quantitatively poor GAC performance in West African environments by *Belward et al.* [1994], subsequent studies have gone onto extract fire count statistics from African GAC data and have used these to parameterize atmospheric chemistry models [e.g., *Cooke et al.*, 1996]. Thus, even in these highly variable ecosystems, GAC-derived statistics have been shown to have significant value.

4. GAC Observations of the 1997 Fire Development

[19] Having established the relative reliability of GAC fire statistics for Borneo in the El Niño year of 1997, the Satellite

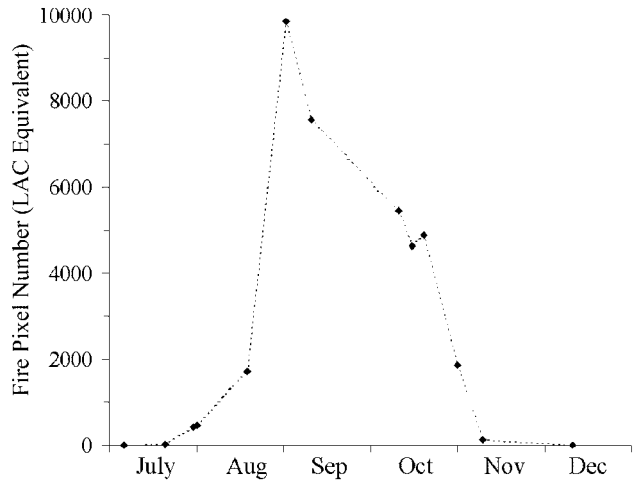

Figure 9. Temporal development of the 1997 Borneo fires as determined using nighttime AVHRR GAC data. Image dates are indicated by data points. Fire pixel numbers are expressed in LAC data equivalent pixels using the inverse GAC sampling procedure, as outlined by *Belward et al.* [1994].

Active Archive was further interrogated to construct a data time series with which to analyze the spatiotemporal development of the 1997 Borneo fires. Relatively cloud free observations were again required, and the archive was found to contain generally two or three suitable nighttime NOAA 14 GAC scenes per month, where Borneo was largely cloud free and located around the center of the AVHRR swath. The selected image dates were 6, 21, and 31 July; 1 and 19 August; 2 and 11 September; 12, 17, and 21 October; 2 and 11 November; and 13 December 1997. The relatively sparse nature of this data set when compared to daily overpass rate of the POES satellite highlights the cloudy nature of this tropical region, even during the intense drought conditions existing in 1997.

[20] Each of the 13 GAC scenes was subject to the fire detection procedure outlined in section 3.2 using a $T_{3.7\text{-}11}$ threshold of 6 K. Fire detection and statistical analyses were carried out using calibrated, raw geometry GAC data, followed by geocoding of the results to indicate temporal changes in fire spatial distribution. Geocoding was carried out using the automatically generated control points present in the AVHRR data header [*Kidwell*, 1995], followed by manual ground control pointing using coastlines. Root-mean-square error in the geocoding was consistently reported as less than one GAC pixel. Geocoded data were compared to the land cover map Forest Cover in Central Indonesia [*World Conservation Monitoring Centre* (*WCMC*), 1996].

[21] Figure 9 shows the variation in fire pixel number as determined from the 13 GAC images listed previously. The data indicate a 3 month temporal envelope for the period of major fires (August–October), with no detectable fires in the 6 or 21 July data and all fires ceasing by 13 December. Unlike the data of *Legg and Laumonier* [1999], only relatively cloud free scenes were used to construct these statistics, but we concur with their finding that the cessation date of the fires appears directly related to the arrival of significant rainfall. This also agrees with the detailed climatic data shown by *Toma et al.* [2000]. Fire activity peaks in the 2 September image, with 9733 LAC pixel equivalent fires identified. The fivefold increase in identified fire pixels between the 19 August and the peak of 2 September highlights this 2 week period as one of the most important in determining the final huge extent of the resulting forest damage. Though they will not be studied here, it is also known that major fires again occurred during the first half of 1998, and in fact, it is believed that forest damage was even greater during this second wave [*Mori*, 2000].

[22] Figure 10shows examples of the geocoded fire pixels extracted from the GAC imagery. At the start of the activity in August 1997 the fires are seen to be active mostly 100–200 km north of the southern coast, an area characterized by the interface

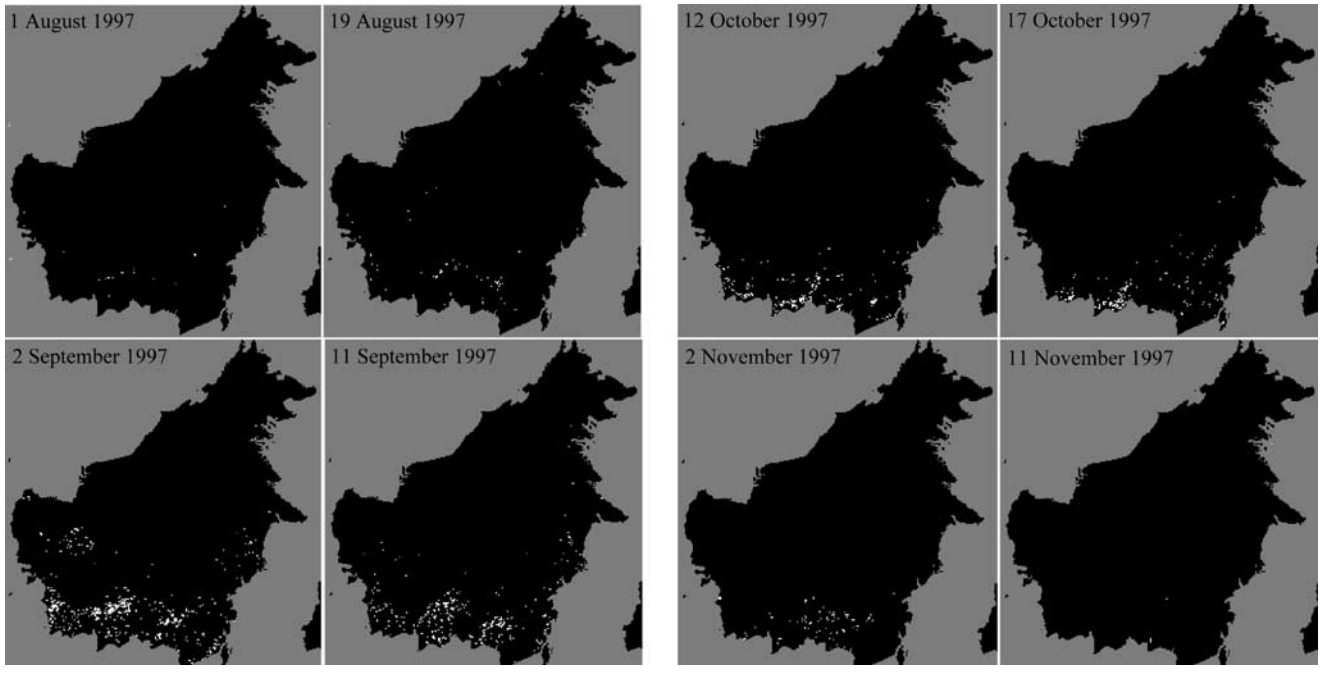

Figure 10. Spatiotemporal evolution of the 1997 Borneo fires illustrated using analysis of eight nighttime AVHRR GAC images of the island taken during the second half of 1997. Each white dot represents a GAC pixel determined to have contained one or more active fires at the time of the satellite overpass.

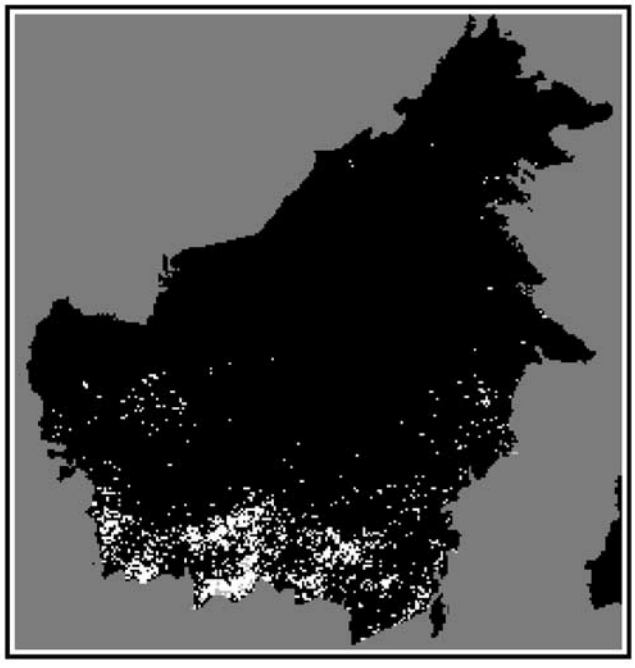

Figure 11. Cumulative map of fire pixels derived from the 13 nighttime AVHRR GAC scenes identified in the data of Figure 9 (July–December 1997). Each white dot represents a GAC pixel determined to have contained at least one active fire at the time of one or more of the satellite overpasses.

between cleared, cultivated land and lowland rain forest. This appears to provide further evidence for the primary cause of the initial fires, namely, land clearance at the forest margin. Over the following months the areas of peak fire concentration move successively southward toward the coast, impacting areas progressively characterized by peat swamp forest [*WCMC*, 1996]. In 1996 this area had been identified as a likely focus for future deforestation by *Achard et al.* [1998], and one region of peak fire activity during September 1997 is concentrated just east of Palangkaraya, an area directly associated with the "Million hectares-Mega-Rice Project" [*Lim et al.*, 1999]. From 1996 this project drained large areas of south Kalimantan's tropical peat swamps using a vast network of canals, with the ultimate but unsuccessful aim of large-scale rice cultivation. The drying and deforestation of the swamp forest associated with this activity most likely acted to directly increase fire intensity in this area. Other fire activity peaks occurred at the same time near the towns of Memala and Panahan in the south and around Ketapang on the eastern coast. The timing of peak fire activity found using GAC imagery concurs with the results of *Nakajima et al.* [1999] and *Legg and Laumonier* [1999], who used data from the Total Ozone Mapping Spectrometer to confirm September 1997 as the period of maximum spatial extent and density of the fire-related haze. Furthermore, *Davies and Unam* [1999] showed that in September 1997 levels of PM_{10} particulates recorded near ground level reached a maximum of 995 $\mu g\ m^{-3}$ as far away as Kuching, Malaysia. This is $\sim$20 times the normal background level, and these concentrations, believed to be the highest ever recorded for an urban area, are directly attributable to the peak in Indonesian fire activity occurring at the time. Interestingly, *Nakajima et al.* [1999] report that the 0.5 μm Angstrom parameters for the haze peaked later, in October 1997,

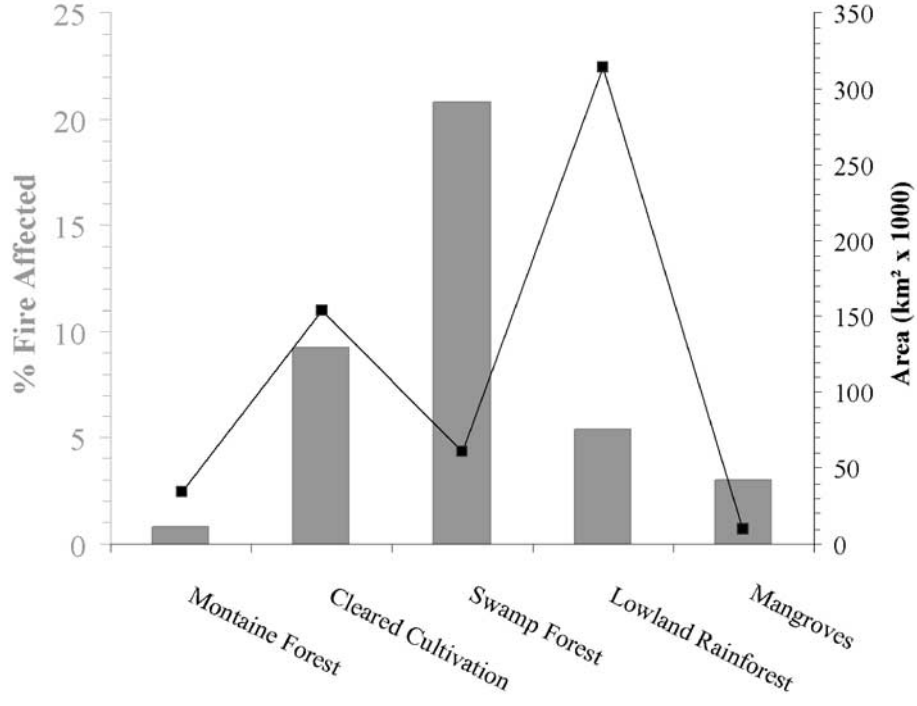

Figure 12. Fire analysis in relation to land cover. Points indicate the area of each respective land cover type identified on the island of Borneo by *WCMC* [1996]. Bars indicate the percentage of each land cover affected by fires according to the cumulative fire pixel map shown in Figure 11.

and one reason maybe the increased burning of peat that occurred as the fires progressed farther into the southern coastal swamps. It seems likely that the smoke from burning peat would have different chemical and particulate characteristics to that produced by burning vegetation, and this may account for the later maxima in the haze optical absorption reported by *Nakajima et al.* [1999].

[23] Figure 11 shows a cumulative fire hot spot map derived from all 13 GAC images. Comparison of this map with the cumulative 1997 ATSR and AVHRR LAC hot spot map of south Kalimantan, included by *Legg and Laumonier* [1999], provides very good agreement, further confirming the legitimacy of the GAC analysis. Comparison with Figure 3 indicates that fires were concentrated in the low-lying areas of Kalimantan, primarily in a latitudinal band below 2°S between Ketapang in the west and Tanahgrogot in the east. Some fire activity is also present in western and eastern Kalimantan, but activity is absent from the central mountain range and from Malaysia and Brunei. The massive impact that the 1997 fires had on south Kalimantan can be clearly perceived from this image. Overlaying this cumulative fire map with the land cover map of *WCMC* [1996] enables a simple calculation of the percentage area of each land cover type that was directly impacted by the 1997 fires (Figure 12). In terms of absolute area, the land cover categories of swamp forest, lowland rain forest, and areas of cleared cultivation were all similarly affected by fire, with only an 8% difference in the number of fire pixels. However, because swamp forest covers a smaller absolute area than these other two land cover types, the percentage of swamp forest impacted by the 1997 fires was far greater, being <20% of the total area of this ecosystem type. The development of such severe fire activity was presumably encouraged by the drying out of the normally moist peat layers during the intense drought, most likely exacerbated by previous draining of large areas in preparation for agriculture. *Siegert and Rücker* [2000] indicate that the postfire survivability of trees in burned swampland was typically far lower than in lowland forest, further highlighting the swampland ecosystem as the most seriously impacted area.

5. Conclusions

[24] This study has shown that useful information on fire number, location, and timing can be obtained from nighttime AVHRR GAC data of Borneo during the intense burning activity that occurred during the second half of 1997. To the extent that analysis of nighttime LAC imagery can be relied upon to produce reliable statistical data [*Eva and Lambin*, 1998; *Legg and Laumonier*, 1999], modeling and comparison of results from simultaneous LAC and GAC imagery have indicated a similar reliability for GAC-derived fire information for this period. Analysis of the 1997 GAC archive confirms that fires commenced in August, primarily in regions of south Kalimantan characterized by the interface between cleared, cultivated land and lowland rain forest. Burning progressed generally southward, with new activity occurring in east and west Kalimantan. Fire activity peaked in September, and all fires were extinguished by December 1997 owing to the November rains. In terms of the percentage of each habitat impacted by the 1997 fires, swamp forests were by far the most severely affected. A new, intense wave of burning began again in early 1998.

[25] GAC analysis of the 1997 fires clearly illustrates the usefulness of this remote sensing data. Though the LAC-to-GAC subsampling process severely degrades the spatial detail of the data derived from GAC imagery, the frequent, long-term coverage make GAC data attractive for time series analysis and for historical studies. The 1997 fires analyzed here are known to be the most intense and widespread to occur on the island of Borneo since 1982–1983, when a previous El Niño-related drought also led to widespread fires that were depicted using GAC imagery [*Malingreau et al.*, 1985]. Further work needs to be carried out to investigate the robustness of the GAC-derived fire information during periods of lower burning intensity when fire sizes and, perhaps, temperatures are likely to be depressed below those of 1997. If such analyses confirm the method to be robust, then decadal-scale variations in fire activity and related environmental change can be reliably investigated using these data.

[26] **Acknowledgments.** M. Wooster is supported in part by the Natural Environment Research Council (NERC) Earth Observation Science Initiative. Three anonymous reviewers are thanked for their insightful and very helpful comments that improved the content and clarity of this manuscript. All AVHRR data used in this paper were obtained from the NOAA Satellite Active Archive. Land cover data of Borneo were obtained from the World Conservation Monitoring Centre, Cambridge, UK.

References

Achard, F., H. D. Eva, A. Glinni, P. Mayaux, H.-J. Stibig, and T. Richards, *Identification Of Deforestation Hot Spot Areas In The Humid Tropics*, *TREES Publications Ser. B*, *Res. Rep. 4*, Eur. Comm., Luxembourg, 1998.

Barbosa, P. M., J.-M. Grégoire, and J. M. C. Pereira, An algorithm for extracting burned areas from time series of AVHRR GAC data applied at a continental scale, *Remote Sens. Environ.*, *69*, 253–263, 1999a.

Barbosa, P. M., D. Stroppiana, J.-M. Grégoire, and J. M. C. Pereira, An assessment of vegetation fire in Africa (1981-1991): Burned areas, burned biomass, and atmospheric emissions, *Global Biogeochem. Cycles*, *13*, 933–950, 1999b.

Belward, A. S., P. J. Kennedy, and J.-M. Grégoire, The limitations and potential of AVHRR GAC data for continental scale fire studies, *Int. J. Remote Sens.*, *15*, 2215–2234, 1994.

Breaker, L. C., Estimating and removing sensor-induced correlation from advanced very high resolution radiometer satellite data, *J. Geophys. Res.*, *95*, 9701–9711, 1990.

Brown, N., Out of control: Fires and forestry in Indonesia, *Trends Ecol. Evol.*, *13*, 41, 1998.

Buongiorno, A., O. Arino, C. Zehner, P. Colarande, and P. Goryl, ERS-2 monitors exceptional fire event in south-east Asia, *Earth Obs. Q.*, *56*, 1–15, 1997.

Cooke, W. F., B. Koffi, and J.-M. Grégoire, Seasonality of vegetation fires in Africa from remote sensing data and application to a global chemistry model, *J. Geophys. Res.*, *101*, 21,051–21,065, 1996.

Cracknell, A., *The Advanced Very High Resolution Radiometer*, Taylor and Francis, Philadelphia, Pa., 1997.

Davies, S. J., and L. Unam, Smoke-haze from the 1997 Indonesian fires: Effects on pollution levels, local climate, atmospheric CO_2 concentrations, and tree photosynthesis, *For. Ecol. Manage.*, *124*, 137–144, 1999.

Eva, H., and E. F. Lambin, Remote sensing of biomass burning in the tropical regions: Sampling issues and a multisensor approach, *Remote Sens. Environ.*, *64*, 292–315, 1998.

Flasse, S. P., and P. Ceccato, A contextual algorithm for AVHRR fire detection, *Int. J. Remote Sens.*, *17*, 419–424, 1996.

Flasse, S. P., P. Ceccato, I. D. Downey, M. A. Raimadoya, and P. Navarro, Remote sensing and GIS tools to support vegetation fire management in developing countries, *IGARSS'97*, pp. 1569–1572, IEEE Press, Piscataway, N. J., 1997.

Fuller, D. O., and M. Fulk, Comparison of NOAA-AVHRR and DMSP-OLS for operational fire monitoring in Kalimantan, Indonesia, *Int. J. Remote Sens.*, *21*, 181–187, 2000.

Giglio, L., J. D. Kendall, and C. O. Justice, Evaluation of global fire detection algorithms using simulated AVHRR infrared data, *Int. J. Remote Sens.*, *20*, 1947–1985, 1999.

Gutman, G., I. Csiszar, and P. Romanov, Using NOAA/AVHRR products to monitor El Niño impacts: Focus on Indonesia in 1997-98, *Bull. Am. Meteorol. Soc.*, *81*, 1189–1205, 2000.

Justice, C. O., and P. Dowty (Eds.), IGBP-DIS satellite fire detection algorithm workshop technical report, *IGBP-DIS Working Pap. 9*, NASA GSFC, Greenbelt, Md., 1994.

Kaufman, Y. J., C. J. Tucker, and I. Fung, Remote sensing of biomass burning in the tropics, *J. Geophys. Res.*, *95*, 9927–9939, 1990.

Kennedy, P. J., A. S. Belward, and J.-M. Grégoire, An improved approach to fire monitoring in West Africa using AVHRR data, *Int. J. Remote Sens.*, *15*, 2235–2255, 1994.

Kidwell, K., NOAA Polar Orbiter Data Users Guide, Satellite Data Serv. Div., Natl. Oceanic and Atmos. Admin., Washington, D. C., 1995.

Kita, K., M. Fujiwara, and S. Kawakami, Total ozone increase associated with forest fires over the Indonesian region and its relation to the El Niño-Southern Oscillation, *Atmos. Environ.*, *34*, 2681–2690, 2000.

Langaas, S., Temporal and spatial distribution of savanna fires in Senegal and The Gambia, West Africa, 1989-1990 derived from multi-temporal AVHRR night images, *Int. J. Wildland Fire*, *2*, 21–36, 1992.

Langaas, S., A parameterised bispectral model for savanna fire detection using AVHRR night images, *Int. J. Remote Sens.*, *14*, 2245–2262, 1993.

Lee, T. F., and P. M. Tag, Improved detection of hotspots using the AVHRR 3.7 μm channel, *Bull. Am. Meteorol. Soc.*, *71*, 1722–1730, 1990.

Legg, C. A., and Y. Laumonier, Fires in Indonesia, 1997: A remote sensing perspective, *Ambio*, *28*, 479–485, 1999.

Levine, J., The 1997 fires in Kalimantan and Sumatra, Indonesia: Gaseous and particulate emissions, *Geophys. Res. Lett.*, *26*, 815–818, 1999.

Liew, S. C., O. K. Lim, L. K. Kwoh, and H. Lim, A study of the 1997 fires in South East Asia using SPOT quicklook mosaics, paper presented at the 1998 International Geoscience and Remote Sensing Symposium, Int. Geosci. and Remote Sens. Symp., Seattle, Wash., July 6–10, 1998.

Lim, O. K., S. C. Liew, M. Nakayama, K. K. Kwoh, and H. Lim, Forest burn scars study using C-band and L-band SAR imagery, paper presented at 20th Asian Conference on Remote Sensing: Forest Resources, Asian Assoc. of Remote Sens., Hong Kong, 1999. Available at http://www.gisdevelopment.net/aars/acrs/1999.

Malingreau, J. P., G. Stephens, and L. Fellows, Remote sensing of forest fires: Kalimantan and North Borneo in 1982-3, *Ambio*, *14*, 314–315, 1985.

Matson, M., and J. Dozier, Identification of subresolution high temperature sources using a thermal IR sensor, *Photogramm. Eng. Remote Sens.*, *47*, 1311–1318, 1981.

Matson, M., and B. Holben, Satellite detection of tropical burning in Brazil, *Int. J. Remote Sens.*, *8*, 509–516, 1987.

Mori, T., Effects of droughts and forest fires in *dipterocarp* forest in East Kalimantan, in *Rainforest Ecosystems of East Kalimantan: El Niño, Drought, Fire and Human Impacts*, *Ecol. Stud.*, vol. 140, edited by E. Guhardja et al., pp. 29–45, Springer-Verlag, New York, 2000.

Nakajima, T., A. Higurashi, N. Takeuchi, and J. R. Herman, Satellite and ground-based study of optical properties of 1997 Indonesian forest fire aerosols, *Geophys. Res. Lett.*, *26*, 2421–2424, 1999.

Nakayama, M., M. Maki, C. D. Elvidge, and S. C. Liew, Contextual algorithm adapted for NOAA-AVHRR fire detection in Indonesia, *Int. J. Remote Sens.*, *20*, 3412–3415, 1999.

Robinson, J. M., Fire from space—Global fire evaluation using infrared remote-sensing, *Int. J. Remote Sens.*, *12*, 3–24, 1991.

Robinson, J., Fire from space: Global fire evaluation using infrared remote sensing, *Int. J. Remote Sens.*, *12*, 3–24, 1999.

Siegert, F., and A. A. Hoffmann, The 1998 forest fires in east Kalimantan (Indonesia): A quantitative evaluation using high resolution, multi-temporal ERS-2 SAR images and NOAA-AVHRR hotspot data, *Remote Sens. Environ.*, *72*, 64–77, 2000.

Siegert, F., and G. Rücker, Use of multitemporal ERS-2 SAR images for identification of burned scars in south-east Asian tropical forest, *Int. J. Remote Sens.*, *21*, 831–837, 2000.

Schweithelm, J., The fire this time—An overview of Indonesia's forest fires in 1997/98, World Wide Fund for Nature Discussion Paper, WWF Indonesia Programme, Jakarta, Indonesia, 1998.

Toma, T., Marjenah, and Hastaniah, Climate in Bukit Soeharto, East Kalimantan, in *Rainforest Ecosystems of East Kalimantan: El Niño, Drought, Fire and Human Impacts*, *Ecol. Stud.*, vol. 140, edited by E. Guhardja et al., pp. 13–25, Springer-Verlag, New York, 2000.

World Conservation Monitoring Centre (WCMC), Forest cover in central Indonesia: Java, Kalimantan, Sulaweisi showing forest protected areas, Cambridge, UK, 1996.

Wooster, M. J., T. S. Richards, and K. Kidwell, NOAA-11 AVHRR/2-Thermal channel calibration update, *Int. J. Remote Sens.*, *16*, 359–363, 1995.

Wooster, M. J., P. Ceccato, and S. P. Flasse, Indonesian fires observed using AVHRR, *Int. J. Remote Sens.*, *19*, 383–386, 1998a.

Wooster, M. J., D. A. Rothery, and T. Kaneko, Geometric considerations for the remote monitoring of volcanoes: Studies of lava domes using ATSR and the implications for MODIS, *Int. J. Remote Sens.*, *19*, 2585–2591, 1998b.

N. Strub and M. J. Wooster, Department of Geography, King's College London, Strand, London WC2R 2LS, UK. (martin.wooster@kcl.ac.uk)